Comments on "Variations of Joint Integrated Data Association with Radar and Target-Provided Measurements"

DOMENIC GAGLIONE
PAOLO BRACA
GIOVANNI SOLDI
FLORIAN MEYER
AUDUN G. HEM
EDMUND F. BREKKE
FRANZ HLAWATSCH

Recently, a method for including target-provided measurements within a joint integrated probabilistic data association (JIPDA) filter was presented and compared with a belief propagation (BP)-based multitarget tracking method. While the JIPDA-based approach uses multiple kinematic models within an interacting multiple model framework, the BP-based approach uses only a single kinematic model. Here, we present and analyze the results of similar experiments conducted on both simulated and real data. Our results show that the JIPDA-based method tends to outperform the BP-based method when the targets are well-separated and perform sharp maneuvers, whereas the BP-based method outperforms the JIPDA-based method when the targets are closely spaced.

D. Gaglione, P. Braca, and G. Soldi are with the Research Department, NATO Centre for Maritime Research and Experimentation (CMRE), 19126 La Spezia, Italy (e-mail: domenico.gaglione@cmre.nato.int; paolo.braca@cmre.nato.int; giovanni.soldi@cmre.nato.int).

F. Meyer is with the Department of Electrical and Computer Engineering and the Scripps Institution of Oceanography, University of California San Diego, La Jolla, CA 92093, USA (e-mail: flmeyer@ucsd.edu).

A. G. Hem and E. F. Brekke are with the Department of Engineering Cybernetics, Norwegian University of Science and Technology, 7034 Trondheim, Norway (e-mail: audun.g.hem@ntnu.no; edmund.brekke@ntnu.no).

F. Hlawatsch is with the Institute of Telecommunications, TU Wien, 1040 Vienna, Austria (e-mail: franz.hlawatsch@tuwien.ac.at).

I. INTRODUCTION

A. Background

In a recent publication [1], three methods for including target-provided measurements in a joint integrated probabilistic data association (JIPDA) framework were proposed. The framework considered in [1], referred to as VIMMJIPDA filter, combines interacting multiple models (IMM) and a visibility state within the well-established JIPDA filter [2]. The IMM concept, first introduced in [3], allows the use of multiple kinematic models for the tracking of maneuvering targets, while the visibility state indicates whether the tracked target is visible to the sensor or not. A target-provided measurement is an observation produced by a target and made available to the tracking method. This observation usually includes kinematic information, e.g., the target's position and velocity, and additional information such as a unique code identifying the target. The target obtains its own position and velocity through an onboard device, generally a global navigation satellite system (GNSS) transponder, and transmits this information, as well as any other relevant information, to neighboring targets and to a central fusion node. Examples of such systems are the automatic identification system (AIS) for maritime surveillance and vessel collision avoidance [4] and the automatic dependent surveillance broadcast (ADS-B) system for air traffic control [5].

These target-dependent reporting systems differ from classical perception sensors such as radar, lidar, and cameras in several aspects. Firstly, the measurements they produce are asynchronous because they are provided by the targets themselves, and each target can transmit its messages at any time. Secondly, a target-provided measurement cannot be a false alarm because it is not the result of a detection process.[1] Several attempts have been made to fuse target-provided measurements and observations produced by perception sensors. One common approach is to consider the reporting system and the perception sensor as stand-alone assets, and accordingly estimate two separate sets of tracks, which are later fused to form a single set of estimated tracks. This approach, which is known as track-level fusion, has some performance limitations compared to measurement-level fusion techniques [6].

The methods proposed in [1] follow a measurement-level fusion approach and are based on the VIMMJIPDA tracking method. Specifically, three different methods for handling the target-provided measurements are proposed. One of them processes the

---

[1]Nevertheless, target-dependent reporting systems like the AIS can be subject to intentional reporting of false information. However, this is not taken into account in [1] nor in the remainder of this paper.

measurements as they arrive, i.e., sequentially; the others collect the measurements and process them at fixed times. The validity of these approaches is demonstrated both in a simulated maritime scenario and with real data acquired as part of the Autosea project conducted by the Norwegian University of Science and Technology [7], and the performance of the proposed methods is compared with that of the belief propagation (BP)-based tracking method with target-provided measurement fusion capabilities presented in [8], [9]. The setup of both the simulated scenario and the real experiment consists of a single radar sensor and the AIS. It is observed that the particle filter (PF) implementation of the BP-based tracking method (referred to as the BP-PF+AIS method) performs worse than the VIMMJIPDA-based methods and, in some cases, even worse than a radar-only method, i.e., a method that uses only the radar measurements.

B. Contribution

The implementation of the BP-PF+AIS method is not publicly available, which led the authors of [1] to use their own implementation. In this paper, we study the performance of the original implementation of the BP-PF+AIS method used in [8], [9] for a simulated scenario similar to the one described in [1, Sec. VIII-A], as well as on the real dataset provided by the Autosea project [7]. Additionally, we consider the simulated scenario described in [9, Sec. VI-A]. The performance obtained with the original implementation of the BP-PF+AIS method is compared with that obtained with the original VIMMJIPDA method using only the radar measurements [2] and with the sequential method proposed in [1] (to be referred to as VIMMJIPDA+AIS), for which code is available in [10]. We note that the BP-PF+AIS method described in [8], [9] does not use multiple kinematic models. However, a BP-based tracking method using multiple kinematic models that conforms to the general IMM approach is presented in [11]. Therefore, we also evaluate and compare the performance of the BP-PF+AIS method described in [8], [9], properly extended to exploit multiple kinematic models as proposed in [11]; we refer to this version as BP-PF+AIS+IMM method. We will demonstrate that while the BP-PF+AIS and BP-PF+AIS+IMM methods have performance advantages in the case of closely spaced targets, the VIMMJIPDA+AIS method performs better when the targets are well-separated and when they perform sharp maneuvers.

The remainder of this paper is organized as follows: Section II provides a brief description of the VIMMJIPDA, VIMMJIPDA+AIS, BP-PF+AIS, and BP-PF+AIS+IMM methods. Section III presents the results of an experimental comparison of these methods conducted on two simulated scenarios, while in Section IV the performance is compared on a real dataset. Concluding remarks are provided in Section V.

II. BRIEF DESCRIPTION OF THE COMPARED METHODS

The VIMMJIPDA method, derived in [2] as a special case of the Poisson multi-Bernoulli filter, is a variation of the JIPDA filter for multitarget tracking that includes multiple kinematic models and a visibility state, and uses hypothesis enumeration to model the target-measurement data association. Specifically, a single-linkage clustering strategy is used to group targets that share measurements. Then, for groups with less than four targets or less than two measurements, brute-force hypothesis enumeration is performed, whereas Murty's algorithm [12] with a maximum of eight hypotheses is used for all other groups. The VIMMJIPDA+AIS method proposed in [1] builds upon [2] and incorporates target-provided measurements. One important technical detail that enables this is to model target birth as a marked Poisson point process, where the marks are constituted by the unique codes identifying the targets.

The BP-based multitarget tracking methods are described in [13] and references therein. The principle behind these methods is to exploit the statistical independence of certain random variables describing the tracking problem, and to represent these independence relationships by means of a factor graph. Then, using a message-passing algorithm—i.e., the sum-product algorithm—on this factor graph enables an intuitive and computationally efficient approximation of the Bayesian inference needed for target detection and estimation. Fundamental for the derivation of these methods is to properly model and formulate the target-measurement data association. An iterative BP-based algorithm for data association with remarkable performance in terms of convergence and accuracy was proposed in [14]. A common approach to implementing BP-based tracking algorithms for general nonlinear/non-Gaussian kinematic and measurement models is to resort to a PF, as described in [15].

Building upon [13]–[15], a suite of BP-PF methods has been developed recently. The BP-PF+AIS method proposed in [9] extends the previous works to incorporate heterogeneous data. This method fuses sensor measurements and target-provided measurements, e.g., AIS data, by establishing an appropriate likelihood for target-provided measurements and a statistical model for data association. A self-tuning BP-PF method that continuously adapts to time-varying system models is proposed in [11]. This method infers and adapts to an unknown detection probability of the sensors and employs multiple kinematic models in line with the IMM framework. Similar to a construction kit system, BP-based algorithm parts can be combined in a modular manner to achieve desired functionalities and properties. For example, the BP-PF+AIS+IMM method, which is used for comparison in this paper, combines the IMM framework proposed in [11] with the ability
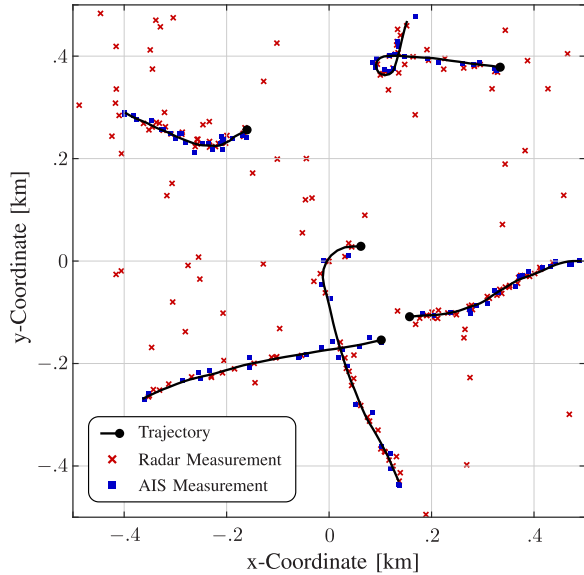
Figure 1. A realization of the simulated scenario considered in [1, Sec. VIII-A], with $P_D = 0.5$. The black dots indicate the final positions of the trajectories.
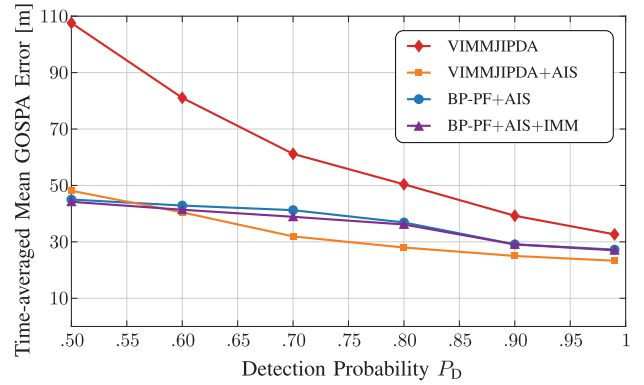

Figure 2. Time-averaged mean GOSPA error versus detection probability P_D of the radar sensor for the simulated scenario considered in [1, Sec. VIII-A].

to fuse sensor measurements and target-provided measurements as established in [9].

III. SIMULATION RESULTS

In this section, we present simulation results for the scenarios considered in [1, Sec. VIII-A] and [9, Sec. VI-A].

A. Scenario Considered in [1]

The simulated scenario considered in [1, Sec. VIII-A] employs a single radar sensor located at $[0,0]^T$ that surveys a circular area of radius 500 m with a time scan duration of 2.5 s. Five targets appear at the edge of that area, three at time $t = 0$ s and two at time $t = 10$ s, initially moving with a velocity of 3.75 m/s. The trajectories of the targets are generated according to a nearly constant velocity (NCV) kinematic model [16, Sec. 6.2.2] with driving noise variance set to 0.1^2 m^2 s^{-3}, and with occasional maneuvers according to a coordinated turn (CT) kinematic model [16, Sec. 4.2.2]. The radar detects a target with probability P_D and generates range-bearing measurements; the measurement noise is a two-dimensional (2D) zero-mean Gaussian random vector with covariance diag(8^2 m^2, 1^2 deg^2). The number of false alarms is Poisson distributed with mean 2. All targets provide AIS measurements containing their unique identifying code as well as their 2D Cartesian position and velocity. The number of AIS measurements provided by a target during each time scan is Poisson distributed with mean 0.5. The AIS measurement noise for position and velocity is a 4D zero-mean Gaussian random vector with covariance diag(3^2 m^2, 3^2 m^2, 0.1^2 m^2/s^2, 0.1^2 m^2/s^2). Figure 1 shows a realization of the scenario

with the trajectories of the five targets, the 2D position component of the AIS measurements, and the radar measurements generated with $P_D = 0.5$.

In Figures 2 and 3, we demonstrate and compare the performance of the radar-only method (i.e., VIMMJIPDA [2]), the sequential method proposed in [1] (i.e., VIMMJIPDA+AIS), the original implementation of the BP-PF+AIS method [8], [9], and the BP-PF+AIS+IMM method. The performance of these methods is measured by the mean generalized optimal sub-pattern assignment (GOSPA) error [17] of order 2 with a cutoff parameter 200 m, averaged over 100 simulation runs. The mean GOSPA error accounts for localization errors for correctly confirmed targets as well as for errors due to missed and false targets. For the VIMMJIPDA and VIMMJIPDA+AIS methods, we use the parameters reported in [1, Tab. III]. Where applicable, the same parameters are also used for the BP-PF+AIS and BP-PF+AIS+IMM methods (e.g., the survival probability), while parameters specifically related to the BP-based methods (e.g., the number of potential targets) are set as in [9]. The VIMMJIPDA and VIMMJIPDA+AIS methods use three models to characterize the kinematics of the targets, namely, two NCV models with different driving noise variances and one CT model. The BP-PF+AIS method uses a single NCV model; therefore, to account for potential maneuvers, the driving noise variance of the NCV model for the BP-PF+AIS method is set to 0.8^2 m^2 s^{-3}. Finally, the BP-PF+AIS+IMM method uses two NCV models with driving noise variance 0.05^2 m^2 s^{-3} and 0.8^2 m^2 s^{-3}. Differently from the NCV model, the CT model does not allow a simple closed-form calculation of the likelihood for the target-provided measurements specified in the supplementary material of [9]. Developing a tractable implementation of this likelihood is outside the scope of this paper, and for this reason, the BP-PF+AIS+IMM method does not employ a CT model.

Figure 2 shows the time-averaged mean GOSPA error when the detection probability P_D of the radar sensor is varied from 0.50 to 0.99. It can be seen that the VIMMJIPDA+AIS method performs better than
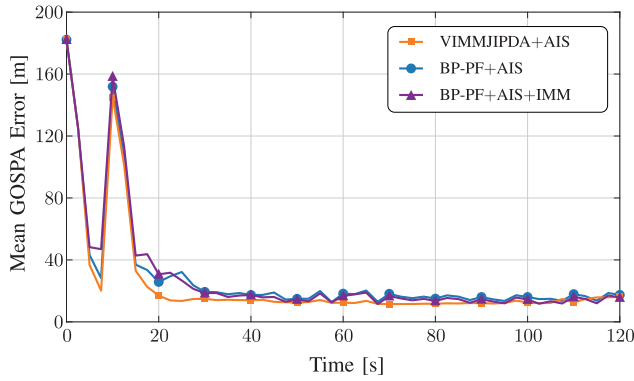
Figure 3. Mean GOSPA error versus time for the simulated scenario considered in [1, Sec. VIII-A] with $P_D = 0.9$.

both the BP-PF+AIS and BP-PF+AIS+IMM methods. Furthermore, the use of multiple NCV models within the BP-PF+AIS method offers only a marginal improvement. The difference in performance between the VIMMJIPDA+AIS method and the BP-PF+AIS and BP-PF+AIS+IMM methods can be explained by the fact that the VIMMJIPDA+AIS method uses also a CT model to better track maneuvering targets, and also by the fact that the BP-PF+AIS and BP-PF+AIS+IMM methods create a larger number of false tracks. However, differently from the results reported in [1], the time-averaged mean GOSPA error of the BP-PF+AIS method is lower than that of the VIMMJIPDA method.

Figure 3 shows the mean GOSPA error versus time for $P_D = 0.9$. Again differently from the results reported in [1], both the VIMMJIPDA+AIS method and the BP-PF+AIS and BP-PF+AIS+IMM methods correctly initialize the targets, as is demonstrated by their similar mean GOSPA errors at times $t = 0$ s and $t = 10$ s, i.e., when the targets appear. The slightly lower mean GOSPA error of the VIMMJIPDA+AIS method relative to the BP-PF+AIS and BP-PF+AIS+IMM methods can again be explained by the fact that the VIMMJIPDA+AIS method uses an additional CT model that allows it to maintain track continuity when targets maneuver and by the larger number of false tracks created by the BP-PF+AIS and BP-PF+AIS+IMM methods. This is confirmed by Table I, which reports the individual costs constituting the mean GOSPA error (averaged over time), i.e., the localization cost for correctly confirmed targets and

Table I
Time-Averaged Individual Costs Constituting the Mean GOSPA Error (in Meter) for the Simulated Scenario Considered in [1, Sec. VIII-A] with $P_D = 0.9$.

	Localization	False	Missed
VIMMJIPDA+AIS	12.3	**0.3**	**12.7**
BP-PF+AIS	12.6	0.8	16.9
BP-PF+AIS+IMM	**11.2**	1.6	17.5

Bold font highlights the lowest value in each column.

Table II
Average Computation Times (in Second) per Time Scan for the Simulated Scenario Considered in [1, Sec. VIII-A].

	P_D					
	0.50	0.60	0.70	0.80	0.90	0.99
VIMMJIPDA	0.32	0.31	0.28	0.28	0.25	0.26
VIMMJIPDA+AIS	0.79	0.70	0.58	0.57	0.45	0.46
BP-PF+AIS	**0.20**	**0.19**	**0.20**	**0.21**	**0.21**	**0.21**
BP-PF+AIS+IMM	0.55	0.53	0.56	0.56	0.56	0.56

Bold font highlights the lowest value in each column.

the costs for missed and false targets. The larger number of false tracks created by the BP-PF+AIS and BP-PF+AIS+IMM methods is mainly due to the use of the heuristic described in [15] to model the generation of new targets, which was later superseded by the fully Bayesian BP-based tracking method proposed in [13].

Finally, Table II presents a comparison between the average computation times per time scan for all the methods. This comparison shows that the BP-PF+AIS method is the fastest method, even faster than the original VIMMJIPDA method that does not process the target-provided measurements. However, definite conclusions cannot be drawn from this analysis, given the different implementations, the different number of kinematic models used, and the different programming languages employed.

B. Scenario Considered in [9]

Next, we present results for a simulated scenario that is similar to the one considered in [9, Sec. VI-A]. Our scenario consists of nine targets that are moving with a constant velocity of 4 m/s. The starting points of the target trajectories are equally spaced on a circle with center $[0, 0]^T$ and a radius of 4 km. The target trajectories and the radar sensor are depicted in Figure 4. Unlike the scenario considered in the previous subsection, here the trajectories are deterministic—thus, they are equal for all simulation runs—and approximately cross each other
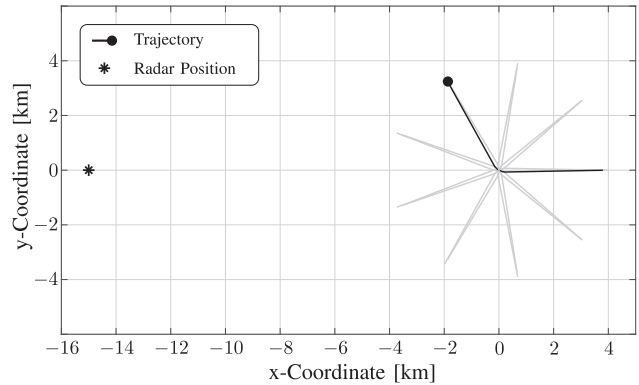

Figure 4. Simulated scenario considered in [9, Sec. VI-A]. The star marks the position of the radar sensor, and the dot indicates the final position of the highlighted trajectory. The other trajectories are rotated (by multiples of 40°) versions of the highlighted one.
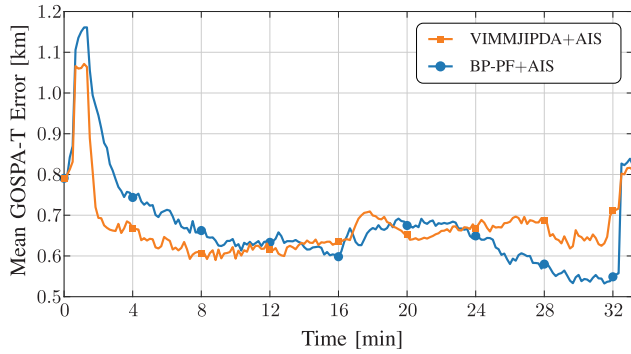
Figure 5. Mean GOSPA-T error versus time for the simulated scenario considered in [9, Sec. VI-A].

	Localization	False	Missed	Switch
VIMMJIPDA+AIS	**249.9**	**138.3**	532.3	**9.5**
BP-PF+AIS	325.0	271.7	**394.8**	10.5

Bold font highlights the lowest value in each column.

in $[0, 0]^{\mathrm{T}}$. Five targets appear at $t = 0$ s and do not disappear, and the other four targets appear at $t = 40$ s and disappear at about $t = 32$ min. Six randomly selected targets provide AIS measurements between $t = 1.5$ min and $t = 31.5$ min. The number of AIS measurements provided by a target during each time scan is Poisson distributed with mean 0.5 for three of the six targets and mean 1 for the other three targets. The time scan duration is set to 10 s. The AIS measurement noise is modeled as before. The radar detects a target with probability $P_{\mathrm{D}} = 0.5$, and it generates range-bearing measurements with a 2D zero-mean Gaussian measurement noise with covariance $\mathrm{diag}(250^2\,\mathrm{m}^2, 2.56^2\,\mathrm{deg}^2)$. The number of false alarms is Poisson distributed with mean 2.

For this scenario, both the BP-PF+AIS and VIMMJIPDA+AIS methods use a single NCV model with driving noise variance set to 0.15^2 $\mathrm{m}^2\,\mathrm{s}^{-3}$. The parameters for the BP-PF+AIS method are set as in [9]. For the VIMMJIPDA+AIS method, we use the parameters reported in [1, Tab. III] with the exception of the clutter density set to 1.7×10^{-9} m^{-2}, the unknown target rate set to 10^{-10} m^{-2}, and the parameters related to the radar measurement noise, that is, the range measurement variance set to 250^2 m^2 and the bearing measurement variance set to 2.56^2 deg^2.

As previously done in [9], we compare the VIMMJIPDA+AIS and BP-PF+AIS methods in terms of the mean GOSPA error for trajectories (GOSPA-T) [18] of order 2 and with a cutoff parameter of 500 m, averaged over 100 simulation runs. Compared to the GOSPA error, the GOSPA-T error additionally accounts for track switches by adding a switching penalty of 125 m. One can see in Figure 5 that the VIMMJIPDA+AIS method outperforms the BP-PF+AIS method during approximately the first half of the simulation, that is, where the targets are well-separated. As the targets get closer, the difference between the GOSPA-T errors of the two methods becomes less significant. From minute 24, after the targets crossed their paths, the BP-PF+AIS method outperforms the VIMMJIPDA+AIS method. This is due to the inability of the VIMMJIPDA+AIS method to continue tracking some of the targets after

they crossed their paths, as demonstrated by the higher time-averaged missed cost component of the mean GOSPA-T error shown in Table III. On the other hand, the time-averaged localization and false costs of the VIMMJIPDA+AIS method are lower than those of the BP-PF+AIS method. In terms of average computation time, the BP-PF+AIS method is faster than the VIMMJIPDA+AIS method: it requires 0.61 s to process each time scan, whereas the VIMMJIPDA+AIS method requires 0.81 s.

IV. RESULTS FOR REAL DATA

Finally, we assess and compare the performance of the VIMMJIPDA, VIMMJIPDA+AIS, and BP-PF+AIS methods for a real dataset that was acquired as part of the Autosea project [7]. The scenario now consists of a radar sensor mounted onboard a semi-autonomous surface craft and four unknown targets: a 30-m-long slow-moving vessel consistently providing AIS measurements and three fast-moving rigid-hull inflatable boats (RHIBs), one of which provides a single AIS measurement. The VIMMJIPDA and VIMMJIPDA+AIS methods employ three kinematic models as in [1]—two NCV models and one CT model—and use the parameters reported in [1, Tab. III]. The BP-PF+AIS method uses a single NCV model with driving noise variance set to 1.7^2 $\mathrm{m}^2\,\mathrm{s}^{-3}$, which is higher than the driving noise variances used for the VIMMJIPDA and VIMMJIPDA+AIS methods, and also noticeably higher than the driving noise variance used for the BP-PF+AIS method in [1]. Results obtained with the BP-PF+AIS+IMM method using two NCV models are not reported because they are equivalent to those obtained with the BP-PF+AIS method.

Figure 6 shows the trajectories estimated by the three methods as colored solid lines. The semiautonomous surface craft is sailing from north to south, and its trajectory, depicted as a gray solid line, is known. The unknown targets are traveling from south to north. The ground-truth trajectory of the slow-moving vessel, obtained by connecting its AIS measurements, is also depicted as a red dashed line; the ground-truth trajectories of the three fast-moving RHIBs are not available. Differently from the results reported in [1], Figure 6 shows that the BP-PF+AIS method performs better than the VIMMJIPDA method, which loses track of one of the three RHIBs when their paths cross, and
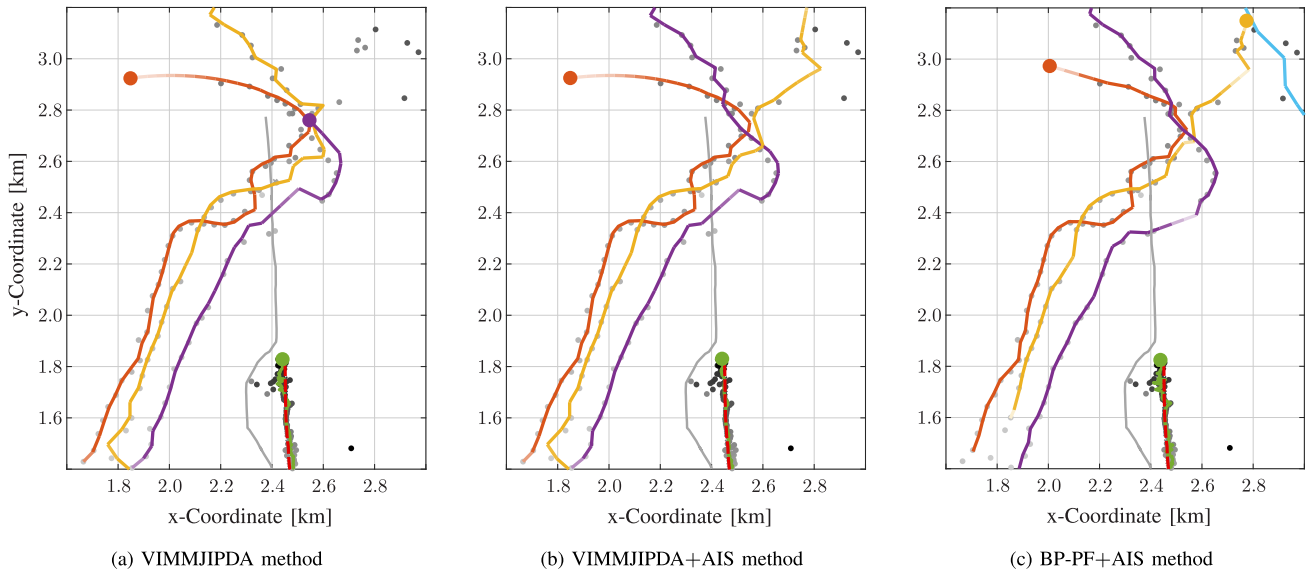
Figure 6. Trajectories estimated by (a) the VIMMJIPDA method, (b) the VIMMJIPDA+AIS method, and (c) the BP-PF+AIS method using a real dataset acquired as part of the Autosea project [7]. The estimated trajectories are depicted in orange, yellow, purple, and green, with their final positions indicated by large dots. The transparency of the tracks is related to their existence probability: lighter (darker) colors correspond to lower (higher) existence probabilities. The red dashed line indicates the ground-truth trajectory of the slow-moving vessel. The gray line represents the known trajectory of the radar sensor. The gray/black dots and crosses indicate the radar and AIS measurements, respectively; the measurements become darker as time passes by. The blue line in the top-right corner of the rightmost panel is a false track created by the BP-PF+AIS method.

performs almost identically to the VIMMJIPDA+AIS method. Despite using only a single NCV model, the BP-PF+AIS method is able to estimate the trajectories of all the targets with high accuracy. The drawbacks of using a higher driving noise variance than the driving noise variances used for the VIMMJIPDA and VIMMJIPDA+AIS methods and for the BP-PF+AIS method in [1] are manifested by the fact that the estimated trajectory for the slow-moving vessel exhibits abrupt changes of direction, and that a false track is created in the top-right corner of the considered area.

V. CONCLUSION

Recently, an extension of the VIMMJIPDA method that is able to include target-provided measurements was proposed in [1]. The effectiveness of this approach was validated in [1] through a comparison with the BP-PF+AIS method presented in [8], [9], whose code is not publicly available. In this paper, we presented the results of an experimental comparison using the implementation of the BP-PF+AIS method originally used in [8], [9], as well as the BP-PF+AIS+IMM method from [11]. Simulation results showed that the VIMMJIPDA+AIS method outperforms the BP-PF+AIS and BP-PF+AIS+IMM methods when the targets are well-separated, whereas the BP-PF+AIS and BP-PF+AIS+IMM methods have performance advantages in the case of closely spaced targets. The reason why the VIMMJIPDA+AIS method performs worse in

the latter case is likely the limited performance of the data association scheme based on Murty's algorithm, which struggles when targets are closely spaced. Improvements to the VIMMJIPDA+AIS method can be obtained by resorting to the variational approximation method presented in [19]. However, due to its use of a CT kinematic model, the VIMMJIPDA+AIS method generally provides more accurate estimates when the targets perform sharp maneuvers. On the other hand, the BP-based data association algorithm used within the BP-PF+AIS and BP-PF+AIS+IMM methods tends to produce better results in challenging tracking environments with tighter target spacings [14]. Finally, results obtained with a real dataset showed that the BP-PF+AIS method using a single NCV kinematic model whose driving noise parameter is sufficiently high can track the agile RHIBs with performance comparable to that obtained with the VIMMJIPDA +AIS method.

REFERENCES

[1] A. G. Hem and E. F. Brekke
"Variations of joint integrated data association with radar and target-provided measurements,"
J. Adv. Inf. Fusion, vol. 17, no. 2, pp. 97–115, Dec. 2022.
[2] E. F. Brekke, A. G. Hem, and L.-C. N. Tokle
"Multitarget tracking with multiple models and visibility: Derivation and verification on maritime radar data,"
IEEE J. Ocean. Eng., vol. 46, no. 4, pp. 1272–1287, Oct. 2021.
[3] H. A. P. Blom and Y. Bar-Shalom
"The interacting multiple model algorithm for systems with Markovian switching coefficients,"
IEEE Trans. Autom. Control, vol. 33, no. 8, pp. 780–783, Aug. 1988.

[4] E. Tu, G. Zhang, L. Rachmawati, E. Rajabally, and G.-B. Huang
"Exploiting AIS data for intelligent maritime navigation: A comprehensive survey from data to methodology,"
IEEE Trans. Intell. Transp. Syst., vol. 19, no. 5, pp. 1559–1582, May 2018.

[5] M. Strohmeier, M. Schafer, V. Lenders, and I. Martinovic
"Realities and challenges of NextGen air traffic management: The case of ADS-B,"
IEEE Commun. Mag., vol. 52, no. 5, pp. 111–118, May 2014.

[6] H. Chen, T. Kirubarajan, and Y. Bar-Shalom
"Performance limits of track-to-track fusion versus centralized estimation: Theory and application,"
IEEE Trans. Aerosp. Electron. Syst., vol. 39, no. 2, pp. 386–400, Apr. 2003.

[7] E. F. Brekke *et al.*,
"The Autosea project: Developing closed-loop target tracking and collision avoidance systems,"
J. Phys. Conf. Ser., vol. 1357, pp. 012020, Oct. 2019.

[8] D. Gaglione, P. Braca, and G. Soldi
"Belief propagation based AIS/radar data fusion for multi–target tracking,"
in *Proc. FUSION-18*, Cambridge, UK, 2018, pp. 2143–2150.

[9] D. Gaglione, P. Braca, G. Soldi, F. Meyer, F. Hlawatsch, and M. Z. Win
"Fusion of sensor measurements and target-provided information in multitarget tracking,"
IEEE Trans. Signal Process., vol. 70, pp. 322–336, Dec. 2021.

[10] Online code repository: Variations of joint integrated data association with radar and target-provided measurements. [Online]. Available: https://doi.org/10.24433/CO.4125751.v2

[11] G. Soldi, F. Meyer, P. Braca, and F. Hlawatsch
"Self-tuning algorithms for multisensor-multitarget tracking using belief propagation,"
IEEE Trans. Signal Process., vol. 67, no. 15, pp. 3922–3937, Aug. 2019.

[12] K. G. Murty
"An algorithm for ranking all the assignments in order of increasing cost,"
Oper. Res., vol. 16, no. 3, pp. 682–687, Jun. 1968.

[13] F. Meyer *et al.*,
"Message passing algorithms for scalable multitarget tracking,"
Proc. IEEE, vol. 106, no. 2, pp. 221–259, Feb. 2018.

[14] J. Williams and R. Lau
"Approximate evaluation of marginal association probabilities with belief propagation,"
IEEE Trans. Aerosp. Electron. Syst., vol. 50, no. 4, pp. 2942–2959, Oct. 2014.

[15] F. Meyer, P. Braca, F. Hlawatsch, and P. Willett
"A scalable algorithm for tracking an unknown number of targets using multiple sensors,"
IEEE Trans. Signal Process., vol. 65, no. 13, pp. 3478–3493, Jul. 2017.

[16] Y. Bar-Shalom, X. R. Li, and T. Kirubarajan
Estimation with Applications to Tracking and Navigation. New York, NY, USA: Wiley, 2001.

[17] A. S. Rahmathullah, Á. F. García-Fernández, and L. Svensson
"Generalized optimal sub-pattern assignment metric,"
in *Proc. FUSION-17*, Xi'an, China, 2017, pp. 1–8.

[18] Á. F. García-Fernández, A. S. Rahmathullah, and L. Svensson
"A metric on the space of finite sets of trajectories for evaluation of multi-target tracking algorithms,"
IEEE Trans. Signal Process., vol. 68, pp. 3917–3928, Jun. 2020.

[19] J. Williams
"An efficient, variational approximation of the best fitting multi-Bernoulli filter,"
IEEE Trans. Signal Process., vol. 63, no. 1, pp. 258–273, Jan. 2015.

Domenico Gaglione (Member, IEEE) received the B.Sc. and M.Sc. degrees (summa cum laude) in telecommunications engineering from Università degli Studi di Napoli Federico II, Naples, Italy, in 2011 and 2013, respectively, and the Ph.D. degree from the Department of Electronic and Electrical Engineering, University of Strathclyde, Glasgow, UK, in 2017. He is currently a Research Scientist with NATO STO Centre for Maritime Research and Experimentation (CMRE), La Spezia, Italy. His research interests include statistical signal processing with emphasis on state estimation, data fusion, and multisensor multitarget tracking.

Paolo Braca (Senior Member, IEEE) received the Laurea degree (summa cum laude) in electronic engineering and the Ph.D. degree (Hons.) in information engineering from the University of Salerno, Fisciano, Italy, in 2006 and 2010, respectively. In 2009, he was a Visiting Scholar with the Department of Electronics and Communication Engineering, University of Connecticut, Storrs, CT, USA. From 2010 to 2011, he was a Postdoctoral Associate with the University of Salerno. In 2011, he joined the NATO STO CMRE, where he is currently a Senior Scientist and a Project Manager. He conducts research in the general area of statistical signal processing with emphasis on detection and estimation theory, wireless sensor network, multi-agent algorithms, target tracking and data fusion, adaptation and learning over graphs, radar (sonar) signal processing, and machine learning. He has coauthored more than 200 publications in international scientific journals, conference proceedings, and NATO technical reports.

Giovanni Soldi received the master's degree in applied mathematics from the University of Milan, Milan, Italy, in 2011, and the Ph.D. degree in signal processing from Télécom ParisTech, Paris, France, in 2016. Since 2016, he has been a Scientist with the Centre for Maritime Research and Experimentation (CMRE), La Spezia, Italy. His research interests include statistical signal processing with a focus on state estimation, data fusion, and multisensor-multitarget tracking techniques.

Florian Meyer (Member, IEEE) received the M.Sc. and Ph.D. degrees (with highest honors) in electrical engineering from TU Wien, Vienna, Austria in 2011 and 2015, respectively. He is an Assistant Professor with the University of California San Diego, La Jolla, CA, jointly between the Scripps Institution of Oceanography and the Electrical and Computer Engineering Department. From 2017 to 2019, he was a Postdoctoral Fellow and Associate with the Laboratory for Information & Decision Systems at the Massachusetts Institute of Technology, Cambridge, MA, and from 2016 to 2017, he was a Research Scientist with the NATO Centre for Maritime Research and Experimentation, La Spezia, Italy. Prof Meyer's research interests include statistical signal processing, high-dimensional and nonlinear estimation, inference on graphs, machine perception, and graph neural networks.

Audun Gullikstad Hem received his M.Sc. in Engineering Cybernetics from the Norwegian University of Science and Technology (NTNU) in 2021, and is currently a Ph.D. student at the Department of Engineering Cybernetics at NTNU. He specializes in target tracking for autonomous surface vehicles, and is currently working in the Autosit project.

Edmund Brekke (Senior Member, IEEE) received the M.Sc. degree in industrial mathematics in 2005, and the Ph.D. degree in engineering cybernetics in 2010, both from the Norwegian University of Science and Technology (NTNU), Trondheim, Norway. From 2010 to 2014, he worked with the Acoustic Research Laboratory (ARL), NUS in Singapore as a postdoctoral Research Fellow. In 2014 he rejoined NTNU and the Department of Engineering Cybernetics, and is currently a Professor in sensor fusion. Brekke's research interests are in the area of sensor fusion and situational awareness, with a particular focus on multi-target tracking and maritime surface autonomy.

Franz Hlawatsch received the Diplom-Ingenieur, Dr. techn., and Univ.-Dozent (habilitation) degrees in electrical engineering/signal processing from TU Wien, Vienna, Austria, in 1983, 1988, and 1996, respectively. Since 1983, he has been with the Institute of Telecommunications, TU Wien, where he is currently an Associate Professor. During 1991–1992, as a recipient of an Erwin Schrödinger Fellowship, he spent a sabbatical year with the Department of Electrical Engineering, University of Rhode Island, Kingston, RI, USA. In 1999, 2000, and 2001, he held one-month Visiting Professor positions with INP/ENSEEIHT, Toulouse, France and IRCCyN, Nantes, France. He (co)authored a book, three review papers that appeared in the IEEE Signal Processing Magazine, about 260 refereed scientific papers and book chapters, and three patents. He coedited three books. His research interests include statistical signal and data processing methods and their application to inference and learning problems.